# Self-Consistent-Field Description of n -Alkanes in Bulk and at the Liquid–Vapor Interface

**ARTICLE** *in* THE JOURNAL OF PHYSICAL CHEMISTRY · FEBRUARY 1996

Impact Factor: 2.78 · DOI: 10.1021/jp9504635 · Source: OAI

# Self-Consistent-Field Description of *n*-Alkanes in Bulk and at the Liquid−Vapor Interface

**Luc J. M. Schlangen, Luuk K. Koopal,* and Johannes Lyklema**

*Department of Physical and Colloid Chemistry, Wageningen Agricultural University, Dreijenplein 6, 6703 HB Wageningen, The Netherlands*

*Received: February 16, 1995; In Final Form: November 1, 1995*[⊗]

A self-consistent-field (SCF) lattice theory for chain molecules in inhomogeneous systems is used to investigate the physical and thermodynamic properties of *n*-alkane liquid−vapor (LV) interfaces. The bulk vapor and liquid phase, where the SCF theory reduces to the Flory−Huggins theory, are studied to obtain a reliable set of parameters. The model fluid is considered as a mixture of (chain) molecules and monomeric vacancies. Intermolecular interactions are described in terms of Flory−Huggins (FH) $\chi$ parameters. The most simple set of parameters is attained when each carbon atom of the linear alkane is considered as a segment with a volume of 0.027 nm$^3$ and the value of $\chi_{AO}$ is taken inversely proportional to the temperature $T$ in kelvin according to $580/T$. On the basis of these two parameters, the theory predicts both *n*-alkane bulk properties such as vapor pressures, density, and heat of vaporization, and properties of the liquid−vapor interface quite reasonably. Volume fraction profiles of the *LV* interfacial region reveal that chain ends are the major constituent of the vapor side of the interface. For longer chains and lower temperatures the relative preference of the chain ends to protrude into the vapor phase is more pronounced. The scaling of the *LV* interfacial tension of *n*-alkanes with increasing molecular weight is correctly predicted. The calculated variation of the *n*-alkane *LV* interfacial tension ($\gamma$) with temperature agrees quantitatively with experimental data. At temperatures close to 0 K, the theory predicts the occurrence of positive $d\gamma/dT$ values (surface freezing).

## Introduction

Detailed knowledge of the structure and thermodynamic properties of interfaces contributes to a better understanding of interfacial phenomena such as adsorption, adhesion, and wetting. As alkanes are important in many practical applications of adhesion and wetting, there is a need for a theory capable of describing the interfacial properties of fluids composed of chain molecules. Such a theory should also be suited to describe the bulk properties of the fluid phases separated by the interface. In principle both lattice theories and Monte Carlo or molecular dynamics simulations are useful for this purpose.

Lattice theories, having relatively low computational costs, have been applied quite successfully to investigate a variety of homogeneous and inhomogeneous systems. Descriptions are provided for, e.g., liquid mixtures and liquid interfaces,[1] polymer melts and solutions,[2] homo and hetero polymer adsorption at solid-liquid interfaces,[3] grafted layers,[3] lipid bilayers,[4] and surfactant behavior in solution[5] and at interfaces.[6]

The description of gaseous phases and liquid/vapor interfaces by lattice theories has been explored by, e.g., Sanchez and co-workers[7,8] and Theodorou.[9] Sanchez et al. have given an accurate description of the vapor pressure, the density, and the interfacial tension of pure alkanes. However, in this approach the parameters of the alkane segments (such as volume and interactions) varied from *n*-alkane to *n*-alkane. This leads to a large the number of parameters when alkanes in general or alkane mixtures have to be described and predictions regarding chain length effects are impossible. Theodorou[9] has investigated the alkane liquid−vapor interface while neglecting the presence of molecules in the vapor phase. In a more elegant description both bulk liquid and bulk vapor should be taken into account, especially when a future aim is to also describe phenomena like alkane vapor adsorption to a solid interface.

An alternative way to describe the properties of hydrocarbons is by Monte Carlo and molecular dynamics simulations. Monte Carlo simulations of *n*-alkanes have yielded, e.g., phase diagrams[10] and heats of vaporization[11] that are in good agreement with experimental data. Such simulations also provide a useful model for the determination of the critical properties of long chain alkanes.[10,12] For the description of interfacial properties Monte Carlo or molecular dynamics simulations are complicated, but Madden[13] has been able to successfully describe the molecular structure of polymer melt−gas interfaces using MC simulations. Harris[14] has described the liquid−vapor interface for decane and eicosane using MD simulations.

In the present paper the self-consistent-field (SCF) lattice theory, developed by Scheutjens and Fleer[15,16] generalized by Evers et al.[17]and discussed in ref 3 will be used to describe both bulk (liquid and vapor) and interfacial properties of *n*-alkanes. This SCF theory is designed to study thermodynamic quantities of inhomogeneous systems, but it can easily be extended to study homogeneous systems. In that case the theory reduces to the multi component Flory−Huggins lattice theory.[2] In the SCF theory alkane fluids are described as a binary mixture of chains and free-volume entities, the vacancies. In contrast to the work of Sanchez et al.[7,8] the segments of the chains will be considered to be identical for all *n*-alkanes. In this way the theory can describe physical properties of *n*-alkanes as a function of chain length and temperature with only a few parameters. Our aim is not directed to a quantitative improvement of the work of Sanchez et al. but to show that even with a very limited parameter set reasonable agreement can be found with experimental data. Advantages of the present approach are that (1) trends become clear and (2) the description to, e.g., branched alkanes, alkane mixtures, and vapor adsorption and wetting of alkane fluids can be done with the same parameter set.

To calibrate the model parameters, the experimental temperature dependence of the vapor pressure will be used. The quality of the parameters will be tested by comparing calculated critical properties, fluid densities, and heats of vaporization with experimental data. As a final aim the interfacial properties of

[⊗] Abstract published in *Advance ACS Abstracts,* February 1, 1996.

0022-3654/96/20100-3607$12.00/0 

*n*-alkanes will be investigated as a function of chain length and temperature. Before we give the results, the SCF theory and the thermodynamic relations used will be briefly introduced.

## Self-Consistent-Field Theory for Chain Molecules in Inhomogeneous Systems

**General Remarks and Outline.** The lattice theory of Scheutjens and Fleer [15,16] was originally developed to describe the equilibrium adsorption of flexible long-chain molecules from solution. The advantage of using a lattice is that the probabilities of chain conformations can be evaluated relatively easy. In the theory always one component (usually the solvent) is used to fill all lattice sites of the system that are not already occupied by the other component(s). In the present situation where pure fluids are considered vacancies are included as the space filling component similarly as was done by Sanchez and Lacombe[7] and Besseling and Scheutjens.[18] Both vapor and liquid phases can be described as a homogeneous mixture of vacancies and fluid molecules composed of a chain of segments. In the interfacial region the system is inhomogeneous and characterized by a gradient in density and potential perpendicular to the interface.

In general, the individual segments of the fluid molecules experience a potential energy that depends on their average surrounding by other segments. Using Boltzmann statistics, the segment volume fractions can be calculated from the potential energies. However, the segment volume fractions, in turn, determine the segment potential energies. Therefore, numerical methods are required to find the self-consistent potential energy field and the corresponding equilibrium segment density profiles. The final volume fraction profiles describe the set of conformations for every type of molecule that corresponds to the minimum Helmholtz energy of the system.

In the theory a lattice fluid system is considered of which each segment or vacancy fills one lattice site. The lattice consists of $M$ parallel layers numbered $z = 1, ..., M$ each with lattice spacing $l$. Each lattice layer contains $L$ lattice sites. By using appropriate boundary conditions fluid−fluid or gas−liquid interfaces can be investigated. The density (or volume fraction) of the segments is considered to be uniform within each lattice layer but variable in the $z$ direction (perpendicular to the interface). Freely jointed chain molecules are modeled with an integer number of segments of type(s) $x$ and/or $y$. Each type of molecule present in the system is denoted by an index $i$, vacancies are distinguished by the index $o$. The total length of the chain molecule equals $N_i$ and the segments are numbered $s = 1, ...., N_i$. The volume fraction of segment $x$ in layer $z$ is given by $\phi_x(z)$. The interaction of segment $x$ with segment $y$ is given by the Flory−Huggins contact interaction parameter $\chi_{xy}$.

The potential energy (with respect to that in the bulk solution) of a free segment $x$ in layer $z$, $u_x(z)$ , is given by[19]

$$u_x(z) = u'(z) + kT\sum\nolimits_y \chi_{xy}(\langle\phi_y(z)\rangle - \phi_y^b) \qquad (1)$$

The potential energy $u'(z)$ is independent of the segment type and accounts for the fact that the sum of all volume fractions in layer $z$ should equal unity. The volume fraction of segment $y$ in the bulk is denoted $\phi_y^b$. The summation term in eq 1 accounts for the contact energies of segment $x$ with its nearest neighbors. The number of contacts of a segment $x$, in layer $z$, with segment $y$ are considered to be proportional to the volume fractions of $y$ in the same and adjacent lattice layers ($z$, $z - 1$ and $z + 1$). The "contact-averaged" volume fraction $\langle\phi_y(z)\rangle$ is given by

$$\langle\phi_y(z)\rangle = \lambda_{-1}\phi_y(z-1) + \lambda_0\phi_y(z) + \lambda_{+1}\phi_y(z+1) \qquad (2)$$

where $\lambda_0$ is the fraction of contacts within the layer $z$, $\lambda_{-1}$ and $\lambda_{+1}$ denote the fractions of contacts in the layers $z - 1$ and $z + 1$, respectively. The values of $\lambda_0$, $\lambda_{-1}$, and $\lambda_{+1}$ depend on the type of lattice used. Usually, the contact fractions affect only the results quantitatively, without affecting qualitative features. In the interfacial region, however, lattice artifacts may appear when the $\lambda$'s differ considerably. To minimize these artifacts $\lambda_0$, $\lambda_{-1}$, and $\lambda_{+1}$ in eq 2 are all set equal to $^1/_3$.

Briefly spoken, the volume fraction of $x$ in layer $z$ is determined by means of a summation over all possible chain conformations. The conformational statistics of the chain molecules are evaluated using a weighted chain extension procedure that adds, one by one, segments to the chain. The probability of each chain extension with a segment $x$ is weighted with a factor $G_x(z)$ defined as

$$G_x(z) = \exp(-u_x(z)/kT) \qquad (3)$$

The weight of a given conformation is found by multiplying the appropriate weighting factors of all segments of a chain molecule while taking into account the connectivity of the chain. The next section describes this procedure in more detail.

**Chain Conformation: First-Order Markov Statistics.** To evaluate the chain statistics of a molecule, it is customary to divide the chain molecule into two chain fragments linked by segment $s$ in layer $z$ and to calculate the so called chain end distribution functions of both fragments. The weighting factor $G_i(z,s|s')$ of a chain fragment $i$ with segment $s$ in layer $z$, where $s$ is linked by a chain of segments to segment $s'$ somewhere in the system, equals $\sum G_i(z,s|z',s')$. The sum is taken over all possible starting positions $z'$. Likewise, $G_i(z,s|1)$ is the weighting factor of an $s$-mer of which the position of the first segment is free and its last segment $s$ is localized in layer $z$, and $G_i(z,s|N)$ is the distribution function for an $(N - s + 1)$-mer with its last segment $s$ in layer $z$ and its first segment $N_i$ free. The distribution functions of the two end fragments of a free chain are generated by "growing" the chain fragments by means of recurrence relations. One chain is generated from segment 1 to $s$, eq 4a, the other from segment $N_i$ to $s$, Eq 4b. The brackets

$$G_i(z,s|1) = G_i(z,s)\langle G_i(z,s-1|1)\rangle \qquad (4a)$$

$$G_i(z,s|N) = G_i(z,s)\langle G_i(z,s+1|N)\rangle \qquad (4b)$$

$\langle\ \rangle$ denote "contact-averaged" distribution functions for the three possible values of $z$, according to

$$\langle G_i(z,s-1|1)\rangle = \lambda_{-1}G_i(z-1,s-1|1) + \lambda_0 G_i(z,s-1|1) + \lambda_{+1}G_i(z+1,s-1|1) \qquad (5)$$

and likewise for $\langle G_i(z,s+1|N)\rangle$. If segment $s$ of molecule $i$ is of type $x$, then $G_i(z,s) = G_x(z)$.

The distribution functions of the chain fragments in eqs 4a and 4b are generated starting from free segments, $s = 1$ and $s = N_i$, respectively, according to

$$G_i(z,1|1) = G_i(z,1) \qquad (6)$$

$$G_i(z,N|N) = G_i(z,N) \qquad \forall\ z$$

The distribution functions 4a and 4b determine the distribution function $G_i(z,s|1;N)$ of chain molecule segment $s$ in layer $z$ provided segment $s$ is part of a chain molecule with the first segment and the last ($N$th) segment anywhere in the system.

The segment volume fraction $\phi(z,s|1;N)$ of $s$ in $z$ now follows from

$$\phi_i(z,s|1;N) = C_i G_i(z,s|1;N) = C_i \frac{G_i(z,s|1)\, G_i(z,s|N)}{G_i(z,s)} \quad (7)$$

where $C_i$ is a normalization constant. To prevent double counting of the linking segment $s$ (present in both chain end fragments), the product of both chain end-point distribution functions is divided by the free segment weighting factor of $s$ in layer $z$. The normalization constant follows from the total amount of segments of component $i$ $\theta_i$ in the system according to

$$\theta_i = \sum_{s=1}^{N_i} \sum_{z=1}^{M} \phi_i(z,s|1;N) \quad (8)$$

For component $i$ with chain length $N_i$, eqs 7 and 8 can be combined to

$$C_i = \frac{\theta_i}{N_i \sum_z G_i(z,N|1)} = \frac{\theta_i}{N_i G_i(N|1)} \quad (9)$$

If not $\theta_i$, but the volume fraction in the bulk $\phi_i^b$ is kept constant the normalization constant is given by

$$C_i = \phi_i^b / N_i \quad (10)$$

The segment density profiles in layer $z$ follow from a summation over all possible values of $s$ within a chain molecule of chain length $N_i$:

$$\phi_i(z) = \sum_{s=1}^{N_i} \phi_i(z,s|1;N) \quad (11)$$

The self-consistent equilibrium volume fraction profile and the corresponding potential energy field are found by numerical methods. Moreover, the partition function is evaluated. This way the mechanical (e.g., pressure and energy) and thermodynamic properties (e.g., enthalpies, interfacial tensions and chemical potentials) of the system can be derived.[4]

**Thermodynamic Relations for Systems with Vacancies.** According to thermodynamics the differential of the Helmholtz energy $F(T,V,A,\{n_i\})$ of a system consisting of two homogeneous bulk phases separated by a flat interface reads

$$\mathrm{d}F = -S\,\mathrm{d}T - p\,\mathrm{d}V + \gamma\,\mathrm{d}A + \sum_i \mu_i\,\mathrm{d}n_i \quad (12)$$

where $S$ is the entropy, $T$ the temperature, $p$ the pressure, and $V$ the volume of the system, $\gamma$ and $A$ are the interfacial tension and the interfacial area, respectively, $\mu_i$ is the chemical potential of a molecule of component $i$, and $n_i$ denotes the number of molecules of component $i$ present in the system. Introducing free volume as component $o$, the volume in a lattice fluid system, $V = \upsilon ML$, is given by the sum of the volumes of all lattice sites that are either occupied by segments or vacancies ($N_o = 1$) according to

$$V = \upsilon \sum_k n_k N_k \quad (13a)$$

where $\upsilon$ is the volume of a lattice site ($\upsilon = l^3$), the index $k$ runs over the molecules $\{i\}$ and vacancies $o$ in the system. In the lattice fluid model $\upsilon$ and $N_k$ are constants, and we have

$$\mathrm{d}V = \upsilon \sum_k N_k\,\mathrm{d}n_k \quad (13b)$$

By substituting eq 13b in eq 12, the latter can be written as

$$\mathrm{d}F = -S\,\mathrm{d}T - p\upsilon \sum_k N_k\,\mathrm{d}n_k + \gamma\,\mathrm{d}A + \sum_i \mu_i\,\mathrm{d}n_i \quad (14)$$

where now $F(T,A,\{n_k\})$. The summation over $k$ can be split into two terms: $k = o$ and $k = i$, and eq 14 reduces to

$$\mathrm{d}F = -S\,\mathrm{d}T - p\upsilon\,\mathrm{d}n_o + \gamma\,\mathrm{d}A + \sum_i (\mu_i - p\upsilon N_i)\,\mathrm{d}n_i \quad (15)$$

By defining

$$-p\upsilon = (\partial F/\partial n_o)_{T,A,\{n_i\}} \equiv \tilde{\mu}_o \quad (16)$$

and

$$\mu_i - p\upsilon N_i = (\partial F/\partial n_i)_{T,A,\{n_{j\neq i}\}} \equiv \tilde{\mu}_i \quad (17)$$

Equation 15 simplifies to

$$\mathrm{d}F = -S\,\mathrm{d}T + \gamma\,\mathrm{d}A + \sum_k \tilde{\mu}_k\,\mathrm{d}n_k \quad (18)$$

According to eqs 16 and 17 the chemical potential of $i$ can now be written as

$$\mu_i = \tilde{\mu}_i - N_i \tilde{\mu}_o \quad (19)$$

The interfacial tension within our system follows, applying standard statistical thermodynamics, from the characteristic function of the grand canonical partition function $\Xi(\{\tilde{\mu}_k\},M,L,T)$ as

$$-kT \ln \Xi(\{\tilde{\mu}_k\},M,L,T) = -kT \ln \Omega(\{n_k\},M,L,U) + U - \sum_k \tilde{\mu}_k n_k = \gamma A \quad (20)$$

where $\Omega(\{n_k\},M,L,U)$ is the microcanonical partition function and $U = TS + \gamma A + \sum_k \tilde{\mu}_k n_k$. Within the SCF theory eq 20 can be transformed to[16]

$$\gamma a/kT = \gamma A/LkT = -\sum_k \theta_k^{\mathrm{exc}}/N_k - \sum_z u'(z)/kT - {}^1/_2 \sum_z \sum_A \sum_B \chi_{AB}(\phi_A(z)\langle\phi_B(z)\rangle - \phi_A^b \phi_B^b) \quad (21)$$

where $a = l^2$ is the lattice cell area, $\theta_k^{\mathrm{exc}} = \theta_k - M\phi_k^b$ and $\phi_k^b$ is the bulk volume fraction of the segment type ($A$ or $B$) or component ($k$) denoted by the subscript.

The chemical potential of the vacancies in a binary mixture of molecules $i$ (with segments $A$ only) and vacancies $o$ follow from the FH theory (ref 2, p 511):

$$\tilde{\mu}_0 = kT(\ln \phi_o^b + (1 - 1/N_i)\phi_i^b + \chi_{AO}(\phi_i^b)^2) \quad (22)$$

Equations 22 and 16 can be combined to find the expression for $p$:

$$p = -\frac{kT}{\upsilon}(\ln \phi_o^b + (1 - 1/N_i)\phi_i^b + \chi_{AO}(\phi_i^b)^2) \quad (23)$$

These expressions can be used to assess the fluid properties.

For binary mixtures two other relations of interest that follow directly from the FH theory are the expressions for the

segment−vacancy interaction and the bulk volume fraction of the polymer segments at the critical point (ref 2, p 544). For $(\chi_{AO})_c$ one finds

$$(\chi_{AO})_c = {}^1/_2(1 + 1/\sqrt{N_i})^2 \tag{24}$$

and for $(\phi_i^b)_c$

$$(\phi_i^b)_c = 1/(1 + \sqrt{N_i}) \tag{25}$$

where the subscript $c$ denotes the lattice fluid critical point. For $\chi_{AO} > (\chi_{AO})_c$ phase separation can occur. Substitution of $(\chi_{AO})_c$ and $(\phi_i^b)_c$ in Eq (23) shows that the pressure at the critical point is solely determined by the chain length and the lattice cell volume.

Finally a note on $\chi_{xy}$. $\chi_{xy}$ is related to the pair contact energies $\epsilon$:

$$\chi_{xy} = Z(2\epsilon_{xy} - \epsilon_{xx} - \epsilon_{yy})/2kT \tag{26}$$

where $Z$ is the coordination number. For the present mixture eq 26 reduces to

$$\chi_{AO} = -Z\epsilon_{AA}/2kT \tag{27a}$$

(by definition, the contact energy for a contact in which a vacancy is involved equals zero). As identical segments attract each other $\epsilon_{AA}$ is negative and $\chi_{AO}$ is positive. In the theory, $\chi$ is considered as purely enthalpic, i.e., its (absolute) magnitude is independent of temperature. Hence, one may write

$$\chi_{AO} = c_2/T \tag{27b}$$

where $c_2$ is a characteristic temperature (expressed in kelvin) equal to $-Z\epsilon_{AA}/2k$. Therefore, only $c_2$ has to be known for the description of the thermodynamic quantities. The critical temperature is found by combining eqs 24 and 27b.

## Results

**Optimal Choice of Parameters.** The elegance of a theory is determined not only by how well it approaches the physical reality but also by the number of parameters needed for the description. In this section two options to arrive at the model parameters will be investigated. The aim is to achieve reasonable results with only a two basic parameters, $c_2$ and $v$, that apply to all alkanes. Intimately related to the choice of these two parameters is the relation between $N_i$ and $C_n$, the number of carbon atoms in the alkane chain. Because of end effects a priori equating $N_i$ to $C_n$ is not necessarily the best choice.

One way to assess the model parameters is through the (saturated) vapor pressure as a function of temperature, see refs 20 and 21 for experimental data. Equations 23 and 27b define the temperature dependence of the lattice fluid pressure. The lattice cell volume follows from the molar mass $M_i$ of component $i$, its density $\rho_i(T)$, and molecular bulk volume fraction $\phi_i^b(T)$ at temperature $T$:

$$v = \frac{M_i\phi_i^b(T)}{N_i\rho_i(T)N_A} \tag{28}$$

According to eqs 27b and 28 the lattice cell volume is defined by the volume fractions $\phi_i^b$ that, in turn, depend on $\chi_{AO}$. To assess $\chi_{AO}$ or $c_2$ from experimental vapor pressure data, a numerical least-squares procedure is required. In the calculations the lattice cell volume for a given alkane is taken independent of temperature and determined by eq 28 using the liquid density at 293 K. Results of the numerical procedure for values of $N_i$ around $C_n$ turn out to be not satisfactory, the lattice cell volumes are *n*-alkane dependent.

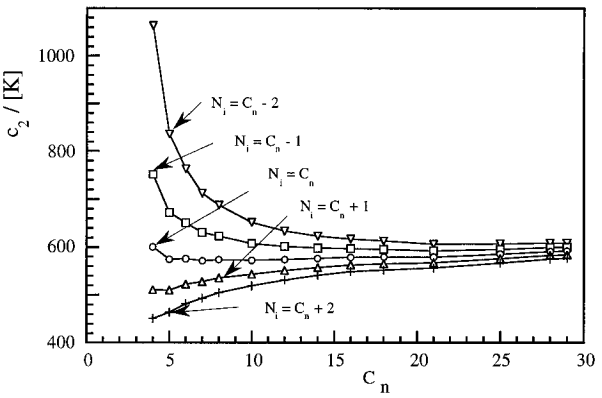


**Figure 1.** Calculated segment−vacancy contact interaction parameter $c_2$ obtained by fitting the theoretical vapor pressure to the experimental pressure at different temperatures[20,21] for $v = 0.027$ nm$^3$. The different choices for $N_i$ to describe the *n*-alkanes are indicated in the figure.

**TABLE 1: Parameter Choice for the Description of *n*-Alkanes with the SCF Theory**[a]

| | |
|---|---|
| $\chi_{AO}$ (kT) | $580/T$ |
| $N_i$ | $C_n$ |
| $v$ (nm$^3$) | 0.027 |
| $a$ (nm$^2$) | 0.09 |
| $T_c$ (K) | $1160/(1 + 1/\sqrt{N_i})^2$ |

[a] The resulting expression for the critical temperature is also given.

In a second option to arrive at consistent parameters the lattice cell volume is fixed. The preliminary calculations indicated that a volume of 0.027 nm$^3$ for a segment is a reasonable choice. With this value of $v$ and taking the experimental vapor pressures as a guideline, the numerical least squares procedure is applied for various relations between $N_i$ and $C_n$, to obtain $c_2$. Resulting $c_2$ values of the *n*-alkanes up to $C_n = 29$, are shown in Figure 1. According to Figure 1 the $c_2$ value approaches a rather constant value of about 580 K if $N_i$ equals $C_n$. The present set of *n*-alkane parameters is considered to be satisfactory and the parameter values are summarized in Table 1. The $a$ value given in Table 1 denotes the lattice cell area, it corresponds to $v^{2/3}$. Also included in Table 1 is the expression for the critical temperature $T_c$, obtained by equating eqs 27b and 24 and using the value of $\chi_{AO}$.

**Bulk Properties of *n*-Alkanes.** In this section the model is used to predict some bulk properties to further test the parameter set shown in Table 1. The calculations are carried out to show that even with a minimum number of parameters reasonably good results can be achieved.

**Vapor Pressures.** As a typical example calculated vapor pressures of *n*-octane and *n*-hexadecane are compared in Figure 2 to experimental data[20,21] for these systems. Figure 2 demonstrates that the theory is able to reproduce, at least semiquantitatively, the temperature dependence of the *n*-alkane vapor pressures. For long *n*-alkanes the agreement is excellent. For short *n*-alkanes the theory underestimates the vapor pressure, especially at more elevated temperatures. For $N_i = 8$, the dotted curve covers a larger temperature range than the solid curve. This implies that the calculated critical temperature is slightly overestimated. Also in this respect better agreement is achieved for longer chains.

**Pressure, Temperature and Density at the Critical Point.** In Figure 3 the calculated pressure at the experimental critical

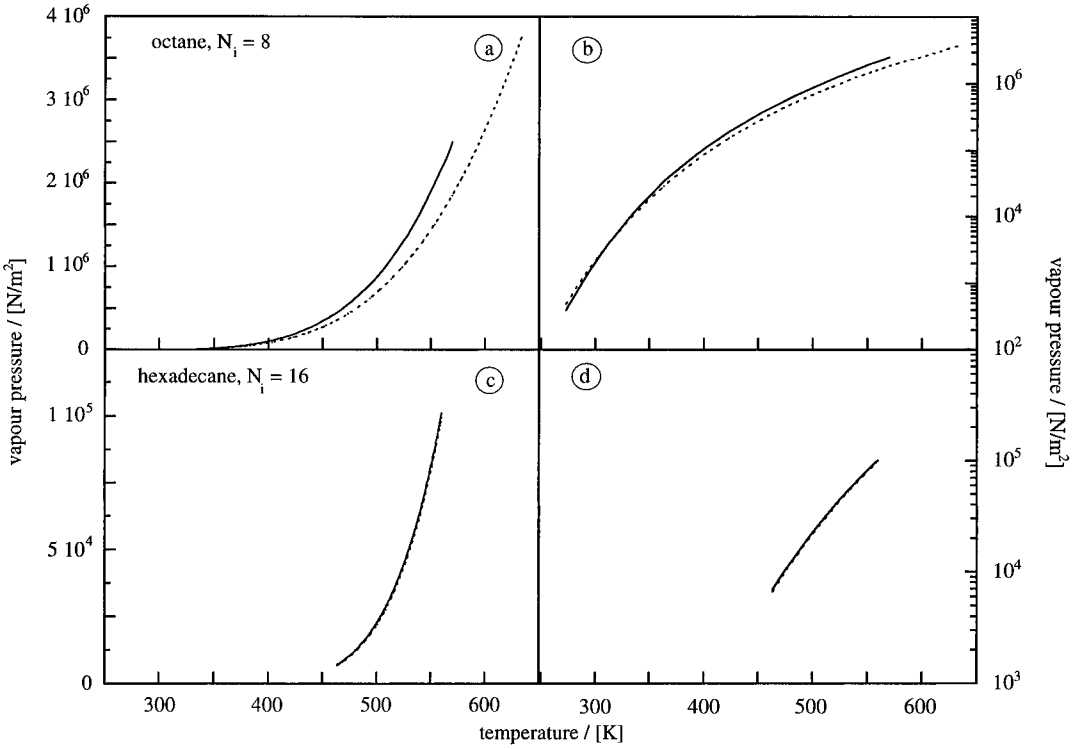


**Figure 2.** Saturated vapor pressures of *n*-octane (a and b) and *n*-hexadecane (c and d). The solid curves are experimental results[20,21] dashed curves are calculated. In panels (a) and (c) the pressure is plotted on a linear scale; in panels (b) and (d) a logarithmic pressure scale is used.

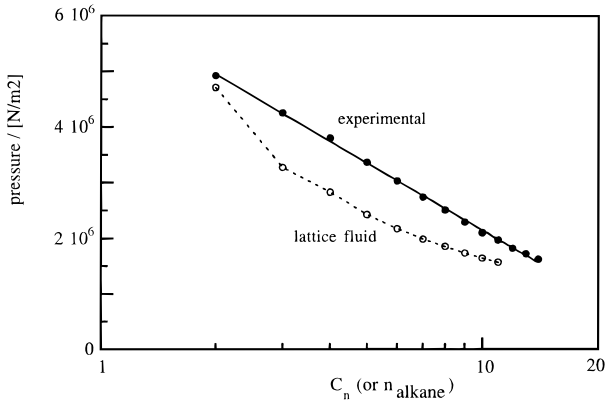


**Figure 3.** Comparison of the calculated pressures (open circles) at the experimental critical temperature with the experimental critical pressure (solid circles)[20] for various *n*-alkanes.

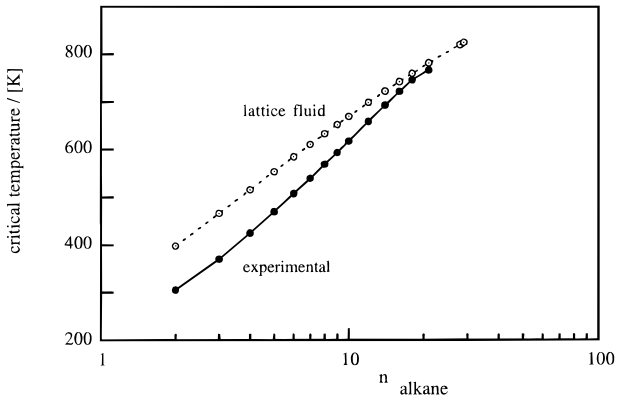


**Figure 4.** Critical temperatures of various *n*-alkanes. The experimental results[20] (solid circles) are compared with the calculated values (open circles).

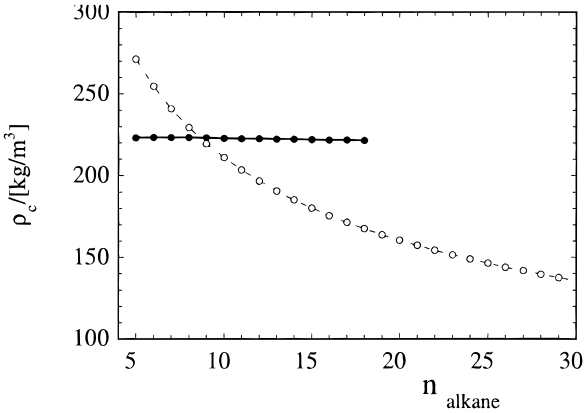


**Figure 5.** Comparison of the calculated (dashed curve) and the measured[23] (solid curve) critical densities in kg/m$^3$ for a series of alkanes.

temperature of the different *n*-alkanes is compared to the experimental critical pressure.[22] The calculated pressures at the (experimental) critical temperature are always somewhat lower than the experimental critical pressures. For chain lengths above 12 the theory is unable to calculate the volume fractions accurately (the value of $\chi_{AO}$ according to eq 27b approaches $(\chi_{AO})_c$).

As noted in relation to Figure 2, the calculated critical temperature does not correspond precisely to the experimental value. In Figure 4 the two are compared, especially for the shorter *n*-alkanes the critical temperatures are overestimated by the lattice fluid theory. For larger *n*-alkanes the agreement is again good. For infinitely large chains, the critical temperature of the lattice fluid (using $c_2 = 580$) attains a plateau value of 1160 K.

A third property that can be investigated is $(\phi_i^b)_c$ or the density at the critical point, $\rho_c$. In Figure 5 both the theoretical and experimental[23] critical density are plotted as a function of chain length. Clearly the theoretical density decreases too much with chain length: for short chains the density is overestimated and for long chains $\rho_c$ is underestimated. Both curves intersect around $C_n = 8$.

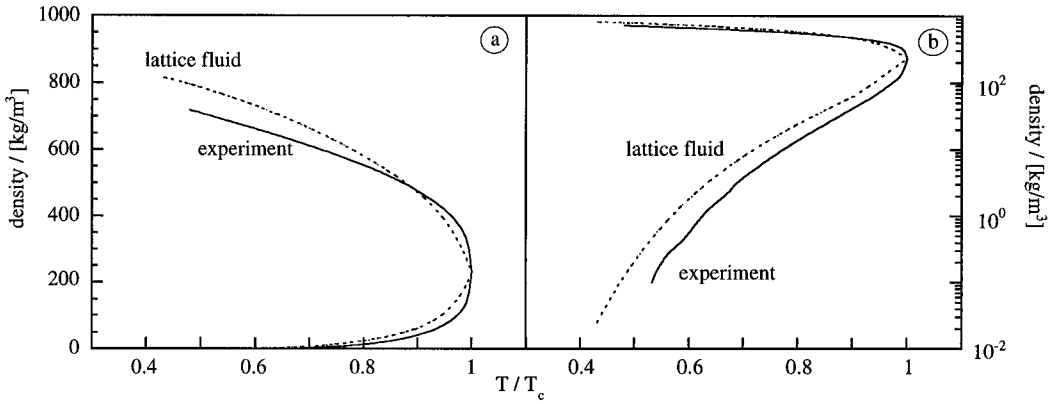


**Figure 6.** Binodal, orthobaric densities of *n*-octane, experimental data[20] (solid curve) are compared with calculated results (dashed curve). In panel (a) the density is plotted on a linear scale, in panel (b) a logarithmic scale is used.

The above results merely serve as an illustration. For a more detailed investigation of the critical point properties the present theory is not appropriate. At the critical point, fluctuations become very large and these are not incorporated in the mean-field approximation.

**Liquid and Vapor Densities.** Both the liquid and vapor density as a function of temperature follow from the volume fractions of the coexisting phases according to eq 28. As an example, the calculated densities of the octameric fluid are shown in Figure 6 and compared to the experimental data of *n*-octane[20]. In panel (a), the density is plotted linearly, in panel (b) semilogarithmically. The theoretical critical temperature of an octamer is 633 K, the experimental critical temperature of *n*-octane equals 569 K. Figure 6 shows that the lattice fluid theory adequately describes both the liquid and vapor densities. Approaching the critical point, the liquid density is underestimated; otherwise, the fluid densities are somewhat overestimated. For longer chains this trend also holds but the critical point is less well predicted, see Figure 5.

**Heat of Vaporization.** The heat of vaporization expresses the enthalpy difference between coexisting liquid and vapor phases. The enthalpy is defined as $H = U + pV$. Within the lattice gas approach, the (configurational) energy $U^b$ of a homogeneous binary mixture bulk phase, consisting of $N_x^\#$ segments $x$ and $N_y^\#$ segments $y$, equals

$$U^b = {}^1/_2 Z(\epsilon_{xx}N_x^\# + \epsilon_{yy}N_y^\#) + N_y^\#\phi_x^b\chi_{xy}kT \qquad (29a)$$

The first term in eq 29a represents the (perfect) configurational energy for random mixing, the second term is the energy contribution due to interactions between unequal segments. For a mixture of alkane segments and vacancies, $\chi_{AO}$ is related to $\epsilon_{AA}$ only (eq 27a), and eq 29a reduces to

$$U^b = -\chi_{AO}N_i n_i \phi_i^b kT \qquad (29b)$$

where $n_i$ is the number of molecules $i$ in the system with energy $U^b$. The molecular energy $u_i^b$ in bulk liquid or vapor of molecules $i$, defined as $u_i^b = U^b/n_i$, therefore equals $-N_i\chi_{AO}\phi_i^b kT$.

The molecular enthalpy $h_i^b$, in bulk liquid or vapor follows from $h_i^b = (U^b + pV)/n_i$. Realizing that $V = n_i N_i v/\phi_i^b$ and making use of eq 16, $h_i^b$ can be calculated as

$$h_i^b = u_i^b - \tilde{\mu}_o N_i/\phi_i^b \qquad (30)$$

The molecular enthalpy of vaporization $\Delta_{vap}/h_i$ is defined as the enthalpy difference between the coexisting bulk vapor and liquid phases (denoted by the superscripts $V$ and $L$, respectively):

$$\Delta_{vap}h_i = h_i^V - h_i^L \qquad (31)$$

The molar heat (enthalpy) of vaporization is obtained as $\Delta_{vap}H_i = N_A\Delta_{vap}h_i$.

In Figure 7 the computed molar heats of vaporization for the homologous series of *n*-alkanes are compared to experimental data.[22] Panel (a) shows the results at 298 K, panel (b) at the normal (1 atm) boiling points. At room temperature, the calculated values tend to be too low. The discrepancy increases with $N_i$. The experimental and theoretical data both depend linearly on the chain length (Figure 7a). At the normal boiling points the enthalpy of vaporization of the *n*-alkanes also increases with increasing chain length (see Figure 7b); however, this increase is smaller than that at room temperature. At the normal boiling points, the calculated heats of vaporization are in quite good agreement with the (extrapolated) experimental values.[22]

In a binary mixture of vacancies and molecules $i$, we have for the Gibbs energy $G = \mu_i n_i$ and $\Delta_{vap}g_i = g_i^V - g_i^L = \mu_i^V - \mu_i^L = 0$. This implies that the molar entropy of vaporization directly follows from $\Delta_{vap}S_i = \Delta_{vap}H_i/T$. The molar entropies of vaporisation corresponding to the enthalpies of Figure 7 are plotted in Figure 8. At room temperature $\Delta_{vap}S_i$ increases with the chain length of the *n*-alkane. However, at the normal boiling points $\Delta_{vap}S_i$ is rather constant for the different chain lengths. Increasing the *n*-alkane chain length raises the boiling temperature and $\Delta_{vap}H_i$ similarly; consequently, $\Delta_{vap}S_i$ is hardly affected. For most fluids, molecules in the vapor phase interact minimally and are in a state of disorder. The differences in $\Delta_{vap}S_i$ of individual fluids may be associated with the internal order in the liquid. Obviously, for *n*-alkanes, the molecular structure at the normal boiling point is rather independent of the alkane chain length.

Summarizing this section, it can be concluded that with only a minimum number of parameters (see Table 1) a very reasonable description of the bulk properties of *n*-alkanes is achieved, especially for long *n*-alkanes.

**Liquid−Vapor Interfacial Properties of *n*-Alkanes.** In this section inhomogeneous systems will be discussed. To investigate the liquid−vapor interface, the size of the system and the amount of molecules and vacancies in the system is chosen such that at each side of the interface a homogeneous bulk phase coexists. The densities of these coexisting phases follow directly from the Flory theory.[2] Without precaution, densities calculated with the SCF theory can deviate from these densities because of the limited size of the system. These artifacts can be eliminated[24] by adjusting the amount of molecules and vacancies in the system and if necessary the size of the system until the

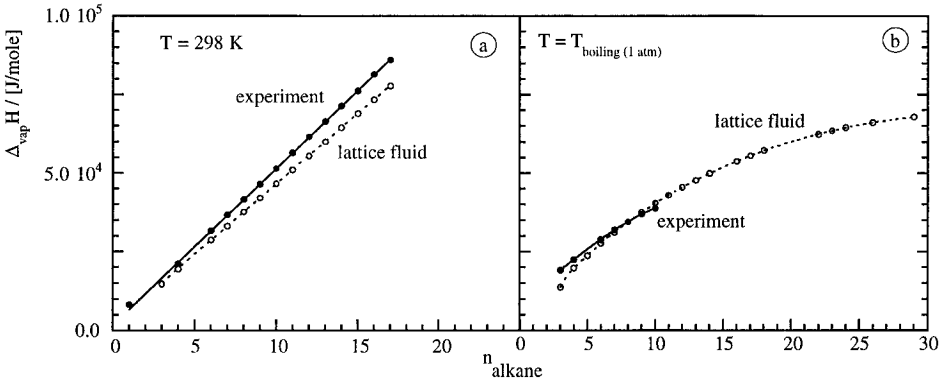


**Figure 7.** Molar enthalpy of vaporisation of different *n*-alkanes. Experimental data (solid points)[22] are compared to calculated results (open circles). In (a) the data at 298 K are plotted against the number of carbon atoms of the *n*-alkane, in (b) the SCF results at the normal boiling points of the *n*-alkanes are compared to (extrapolated) experimental data.

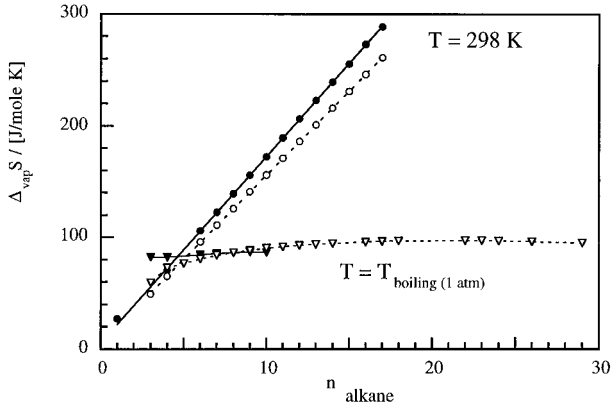


**Figure 8.** Entropy of vaporization for the series of *n*-alkanes shown in Figure 7. Calculated values (open points) are compared to experimental data (solid points) at room temperature (circles) and at the normal boiling temperature (triangles).

volume fractions of the coexisting bulk phases equal those calculated with the Flory theory.

**Volume Fraction Profiles.** The inhomogeneity of the interfacial region is characterized by (1) the segment density distributions or volume fraction profiles in the interfacial region and (2) the position of segments with a given ranking number in the chain. To investigate the behavior of segments with different ranking numbers $s$ in chain $i$ it is convenient to describe the distribution of segments $s$ in chain $i$ relative to the average distribution of segments $i$, i.e., $\phi_i(z,s)N_i/\sum_s\phi_i(z,s)$. If a lattice layer is part of an isotropic phase, the relative segment distributions are unity for any segment. In an inhomogeneous phase accumulation of $s$ is indicated by relative segment densities larger than unity. Both absolute and relative density profiles at the boundary of the coexisting liquid and vapor phases are plotted in Figure 9 for two temperatures and for chain molecules with $N_i = 4$ and $N_i = 8$. The absolute densities are shown at the left, the corresponding relative segment distributions at the right. Note that segments with ranking numbers $s = 1 + x$ and $s = N - x$ have identical volume fraction profiles $\phi_i(z,s)$. In each plot, the liquid phase is positioned at the left hand side, the vapor phase on the right-hand side. The shaded regions in the plots indicate the highest segment and vacancy density gradients between two adjacent lattice layers. The profiles are symmetrical with respect to exchanging molecules and vacancies.

With decreasing temperature, the thickness of the interfacial region (with densities differing from those in the coexisting bulk phases) decreases. At $T = 0$ K any interface becomes a step function. The relative segment distributions (panels b, d, and f) reveal that the chain end segments have a (relative) preference for the vapor side of the interface, whereas the middle segments avoid this region. In a molecular dynamics simulation studies[14,25] and other lattice fluid studies[9] this feature has also been observed. With increasing temperature this behavior becomes less pronounced (compare panels b and d). Increasing the chain length enhances the (relative) preference of the chain ends for the vapor-phase boundary side of the interface (compare panels d and f). The present results show that with an appropriate SCF theory similarly rich structural details can be obtained as with molecular dynamics simulations.[14]

The reason for the difference in interfacial behavior of chain end and middle segments is 2-fold. First, middle segments drag two neighboring segments to the interfacial region, whereas end segments only have one neighboring segment. Thus, when chain ends are exposed to the vapor boundary side of the interface, the number of unfavorable segment−vacancy contacts is smaller. Second, the conformational entropy of a chain molecule in the interfacial region is larger when a chain end is pushed out of the interface instead of a train of segments. These two effects become more pronounced upon decreasing the temperature and increasing the chain length.

**Temperature Dependence of the Interfacial Tension.** The interfacial tension $\gamma$ follows from the density profiles according to eq 21 and is expressed per area of a lattice site. For conversion to units of J/m$^2$ this value has to be multiplied with the lattice cell area $a$, see Table 1. According to general thermodynamics (eq 12) $\gamma$ is related to the Helmholtz energy as

$$\gamma = (\partial F/\partial A)_{T,V,\{n_i\}} = (\partial U/\partial A)_{T,V,\{n_{i,}\}} - T(\partial S/\partial A)_{T,V,\{n_i\}} \quad (32)$$

the second term on the right hand side accounts for the excess interfacial entropy $S^\sigma \equiv (\partial S/\partial A)_{T,V,\{n_i\}}$ and equals $-(\partial\gamma/\partial T)_{V,\{n_i\}}$.

Figure 10a shows the calculated temperature dependence of the interfacial tension for alkanes of various lengths. Upon decreasing the temperature, any fluid will eventually freeze. Application of the SCF theory to describe frozen states has to be performed with care. Therefore, the curves are dashed for temperatures below the freezing temperatures of the *n*-alkanes. For the moment we restrict the discussion to the solid part of the curves. The solid curves show that $(\partial\gamma/\partial T)_{V,\{n_i\}} < 0$, for both monomers and chain molecules, hence $S^\sigma$ is positive. According to the theory, $S^\sigma$ decreases with increasing chain length. Upon increasing the temperature (for a certain chain length), the magnitude of $S^\sigma$ increases until it reaches a maximum (at the inflection point of the $\gamma$ (T) curve). After the maximum $S^\sigma$ decreases with increasing temperature to vanish (together with the phase boundary) at the critical temperature.

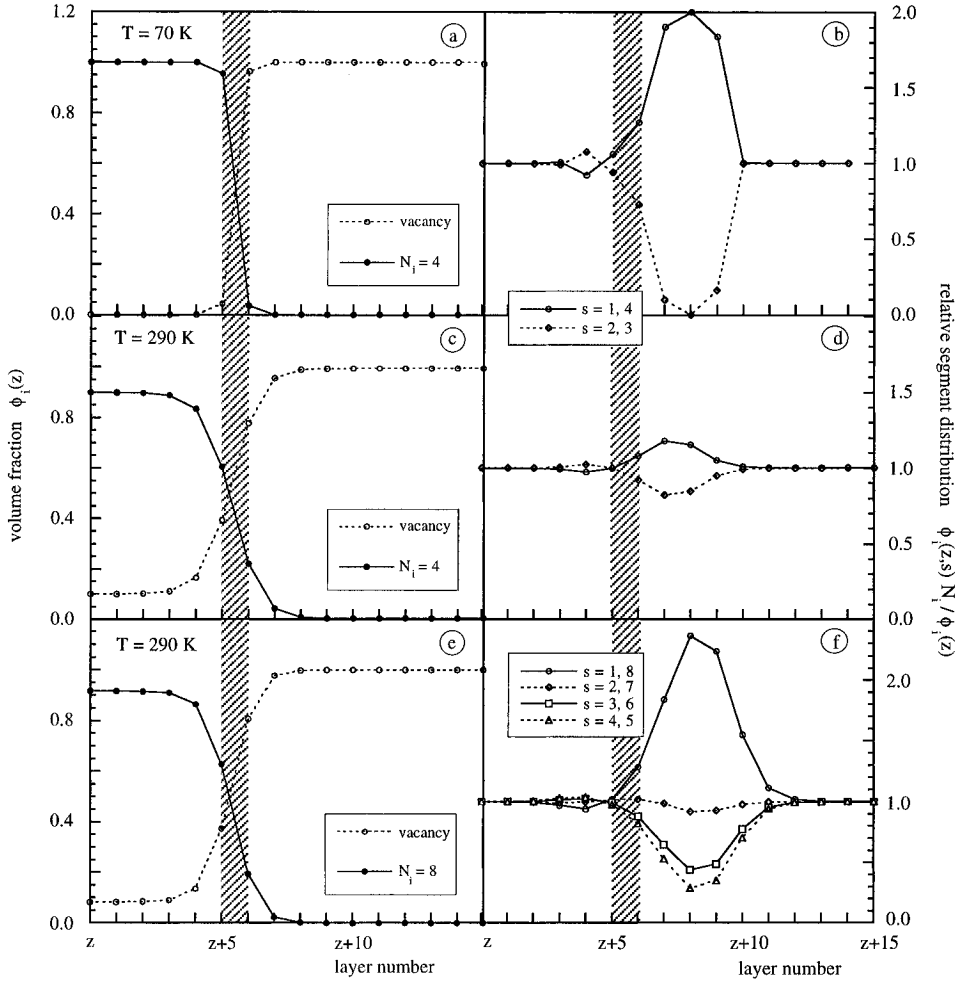


**Figure 9.** Volume fraction profiles (left-hand side) and corresponding relative segment distribution profiles (right-hand side) of the liquid−vapor interfacial region for various temperatures and chain lengths. The layer with the steepest volume fraction decay is shaded.

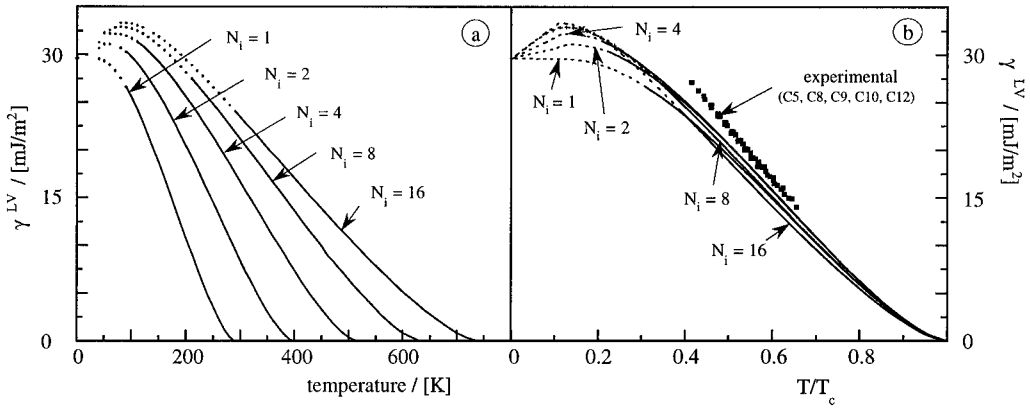


**Figure 10.** Liquid−vapor interfacial tension for liquids of varying chain length as a function of temperature. The drawn curves are the results calculated for temperatures above the melting temperature of the *n*-alkane. Below the melting point only calculated points are shown. In panel (b) the calculated interfacial tensions are plotted against the reduced temperature. Below the melting temperature the curves are dashed. The experimental interfacial tensions for several *n*-alkanes[26] ($C_5$, $C_8$, $C_9$, $C_{10}$, and $C_{12}$) are also shown.

The interfacial excess entropy has two (main) contributions: (1) the excess conformational entropy of the chains at the interface and (2) the excess entropy of mixing vacancies and molecules. For monomeric fluids the conformational contribution at the interface is absent and $S^\sigma$ is solely determined by the mixing term. Thus, the maximum in $S^\sigma(T)$ for the monomeric fluid is a reflection of the temperature dependency of the interfacial excess mixing entropy. The $\gamma$ (T) curves suggest that this conclusion also applies to chain molecular fluids.

In Figure 10b the results of the calculations for *n*-alkanes are plotted against the reduced temperature $T/T_c$. The solid parts of the calculated $\gamma(T/T_c)$ curves are nearly independent of the chain length. The experimental data on the temperature dependency of the interfacial tension for different individual *n*-alkanes[26] are also plotted against the reduced temperature $T/T_c$ in Figure10b. The data merge in an almost linear master curve situated slightly above the calculated results. Note that for a comparison of the calculated and experimental interfacial tensions it should be realized that, usually, experimental data

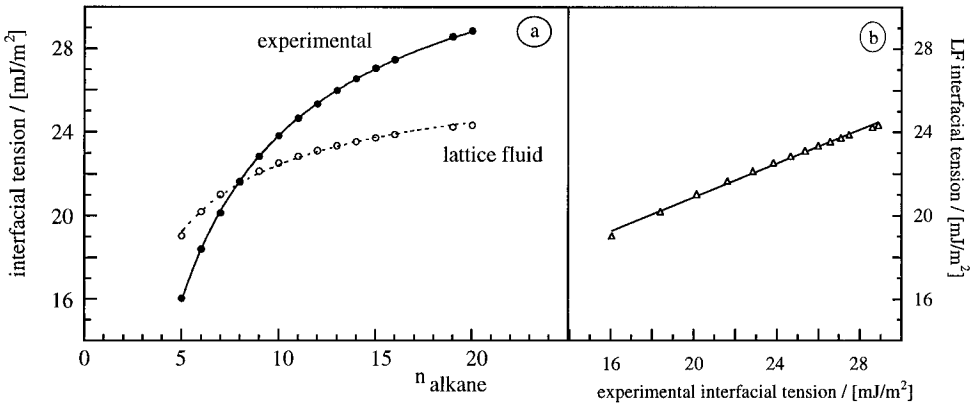


**Figure 11.** Calculated interfacial tensions (open circles) of the liquid−vapor interface of various *n*-alkanes at 293 K compared to experimental data[26] (solid points). In (a) the curves through the points are drawn according to eq 33. In (b) the calculated interfacial tensions are plotted against the experimental ones.

are obtained under an atmosphere of hydrocarbon vapor and dry nitrogen. In the calculations the presence of nitrogen is neglected.

The SCF theory considers molecules to be randomly distributed. Therefore, at low temperatures it describes the interface of a supercooled fluid. Although the model parameters are derived from bulk fluid properties well above the freezing temperatures, it may be interesting to briefly discuss the low-temperature part of the $\gamma(T/T_c)$ plots. At 0 K interfaces are dead sharp (i.e., $\phi_i^V = 0$ and $\phi^S = 1$), in general $S^\sigma$ vanishes and in the SCF theory the interfacial tension is given by the contact fraction with the next layer $\lambda_{+1}$ together with the segment−segment interaction according to $\gamma = \lambda_{+1}c_2k/a$ (as $Z\epsilon_{AA}/2 = c_2k$; see eq 27b), independent of the chain length. Figure 10b shows that for monomers, $\gamma$ only decreases with temperature whereas for chain molecules a maximum interfacial tension is found at $T/T_c \approx 0.12$, rather independent of the chain length. The maximum in the $\gamma(T/T_c)$ curves, if realistic, would imply the occurrence of negative $(\partial S/\partial A)_{T,V,\{n_i\}}$ values around $T/T_c \approx 0.12$. For *n*-alkanes ($C_n > 14$) just above their bulk freezing temperature, the occurrence of negative $S^\sigma$ values (surface freezing) has been observed experimentally.[27,28] A negative $S^\sigma$ means that the entropy of the interfacial region is lower than in the bulk, i.e., the interfacial region has a higher degree of organization than the high-density bulk phase. A physical argument could be that at a sharp interface, the conformational entropy of the molecules in the interface is restricted as compared to that in the bulk phase. This restriction will be more serious for long chains than for short ones. In our calculations the maximum in the $\gamma(T/T_c)$ curve not only occurs for long *n*-alkanes, it is also found for short *n*-alkanes for which surface freezing has not been observed. Furthermore, the $\gamma$ maximum occurs at temperatures below the experimentally established *n*-alkane surface freezing temperatures. These discrepancies have to do with the weakness of the current model parameters to describe frozen phases. Very recently Leermakers and Cohen Stuart[29] have analyzed this problem in more depth by application of the self-consistent anisotropic field scheme within the present model. This scheme accounts for the tendency of densely packed chain molecules to line up.[30]

**Chain Length Dependence of the Interfacial Tension.** Calculated LV interfacial tensions as a function of chain length are compared with experimental data[26] (at $T = 293$ K, under 1 bar of hydrocarbon vapor and dry nitrogen) in Figure 11a. In Figure 11b the calculated results are plotted directly against the experimental values. The experimental surface tensions of the homologous series of *n*-alkanes scale with the molecular weight to the power −2/3.[31] The drawn and dotted curves in Figure 11a are described by the relation

$$\gamma_n = \gamma_{n\to\infty} - k_{alk}/C_n^{2/3} \tag{33}$$

The constants $\gamma_{n\to\infty}$ and $k_{alk}$ (in mJ/m$^2$) corresponding to these curves are 37.3 and 62.5 for the experimental data and 27.9 and 25.4 for the model, respectively. Both eq 33 and Figure 11b imply that the scaling of the calculated interfacial tension with the number of carbon atoms of the *n*-alkane is correctly reproduced. The current results are an important improvement compared to previous efforts to model the chain length dependence of the interfacial tension of the *n*-alkanes[9].

For the short *n*-alkanes the interfacial tension is overestimated. This has to do with end effects: for short chains (especially for $C_n < 8$) the area of a lattice site is underestimated by the value given in Table 1 ($CH_3$ groups are relatively large). This means that the calculated value of the interfacial tension will be too high. For $C_n > 8$ the lattice cell volume is close to 0.027 nm$^3$ and the $a$ value of 0.09 nm$^2$ is correct; yet the lattice fluid theory slightly underestimates the interfacial tension. The difference increases with increasing chain length and eventually, according to the $\gamma_{n\to\infty}$ values, the theory underestimates the interfacial tension of infinitely long chains by 32%. According to Figure 10b, we increasingly underestimate the LV interfacial tension for lower reduced temperatures. With increasing chain length of the *n*-alkane, the critical temperature increases (see Figure 4) and $T/T_c$ at 293 K decreases so that $\gamma$ at 293 K will also be increasingly underestimated.

## Concluding Remarks

The present SCF theory (semi)quantitatively reproduces various bulk and interfacial properties of normal alkanes with a minimum number of adjustable parameters. Optimal predictions of the bulk fluid properties, such as saturated vapor pressure, density, and heat of vaporization, all well between the freezing temperature and the critical temperature, are attained if the *n*-alkane molecules are considered as chains in which each carbon atom is represented as one segment with a volume of 0.027 nm$^3$ and the contact interactions are quantified by $\chi_{AO} = 580/T$ ($T$ in kelvin)

Being satisfied with the bulk fluid description, the same parameter set has been used to calculate of the LV interfacial properties of *n*-alkanes with the SCF theory. Density profiles of the LV interfacial region reveal that chain end segments, protruding into the vapor, are the major constituent of vapor side of the interface. At the liquid side of the interface, chain middle and end segments are equally distributed. The theory

reproduces the chain length dependence and temperature dependence of the *n*-alkane interfacial tensions rather accurately. For $0.4 < T/T_c < 0.8$, the calculated interfacial tension rises linearly with decreasing $T/T_c$. This has also been established experimentally. For the moment experimental data on the interfacial tension of *n*-alkanes for $T/T_c$ values below 0.4 are lacking. In this region the theoretical predictions can be verified experimentally by measuring the LV interfacial tension of shorter *n*-alkanes, which are still liquids below $T/T_c = 0.4$.

If the model is applied beyond the temperature range for which the parameters have been derived, viz., below the *n*-alkane freezing temperatures, positive $d\gamma/dT$ values occur and a maximum in the LV interfacial tension is found at $T/T_c \approx 0.12$. The position of the maximum is virtually independent of the chain length of the molecule. Positive values indicate a highly ordered interface. Experimentally, positive $d\gamma/dT$ values have been established for *n*-alkanes ($14 < C_n < 50$) just above their bulk freezing temperature. Recently the theory has been improved by Leermakers et al.[29] to study surface freezing in more detail.

The parameters used in the calculations have been obtained by comparing calculated and experimental data for homogeneous systems. With homogeneous systems it is relatively straightforward to describe the (infinite range) Lifshits−van der Waals interactions in *n*-alkane bulk fluids with nearest-neighbor interactions. However, for the LV interface with a large difference in density between the L and V phase, this is a more serious approximation. In principle it is possible to include long-range interactions, but this remains a task for the future.

Other shortcomings of the theory that may play a prominent role for relatively small chains as considered here are the too large chain flexibility and the fact that $CH_3$ segments differ in properties from the $CH_2$ segments. Again these shortcomings are more serious for inhomogeneous systems than for homogeneous ones. For inhomogeneous systems these limitations can be improved by introducing respectively an energetic distinction between gauche and trans conformations using the rotational isomeric state scheme[4] and by considering the end segments as separate segments.

The present calculations should be considered as a first survey of the possibilities of the SCF lattice theory to describe LV interfaces. More advanced calculations could include a more complex architecture and or rigidity of the alkane molecules, alkane mixtures and alkanes near solid interfaces. The latter type of calculations are very interesting because they allow insight in wetting phenomena. Some first SCF results on alkane adsorption and surface wetting by alkanes can be found in refs 32−34.

**Acknowledgment.** This work has been supported by the European Union under Contract JouF-0020F(CD).

## References and Notes

(1) Guggenheim, E. A. *Mixtures*; Clarendon: Oxford, 1952.

(2) Flory, P. J. *Principles of Polymer Chemistry*; Cornell University Press: Ithaca NY, 1953.

(3) Fleer, G. J., Cohen Stuart, M. A., Scheutjens, J. M. H. M., Cosgrove, T.; Vincent, B. *Polymers at Interfaces*; Chapman & Hall: Cambridge, 1993.

(4) Leermakers, F. A. M.; Scheutjens, J. M. H. M. *J. Phys. Chem.* **1988**, *89*, 3264−3274.

(5) Böhmer, M. R., Koopal, L. K.; Lyklema, J. *J. Phys. Chem.* **1991**, *95*, 9569−9578.

(6) Böhmer, M. R.; Koopal, L. K. *Langmuir* **1992**, *8*, 2660−2665.

(7) Sanchez, I. C.; Lacombe, R. H. *J. Phys. Chem.* **1976**, *80*, 2353−2362.

(8) Poser, C. I.; Sanchez, I. C. *J. Colloid Interface Sci.* **1979**, *69*, 539−548.

(9) Theodorou, D. N. *Macromolecules* **1989**, *22*, 4578−4589.

(10) Siepmann, J. I., Karaborni, S.; Smit, B. *J. Am. Chem. Soc.* **1993**, *115*, 6465−6455.

(11) Kaminski, G., Duffy, E. M., Matsui, T.; Jorgensen, W. L. *J. Phys. Chem.* **1994**, *98*, 13077−13082.

(12) Smit, B., Karaborni, S.; Siepmann, J. I. *J. Chem. Phys.*, in press.

(13) Madden, W. G. *J. Chem. Phys.* **1987**, *87*, 1405−1422.

(14) Harris, J. G. *J. Phys. Chem.* **1992**, *96*, 5077−5086.

(15) Scheutjens, J. M. H. M.; Fleer, G. J. *J. Phys. Chem.* **1979**, *83*, 1619−1635.

(16) Scheutjens, J. M. H. M.; Fleer, G. J. *J. Phys. Chem.* **1980**, *84*, 178−190.

(17) Evers, O. A., Scheutjens, J. M. H. M.; Fleer, G. J. *Macromolecules* **1990**, *23*, 5221−5232.

(18) Besseling, N. A. M.; Scheutjens, J. M. H. M. *J. Phys. Chem.* **1994**, *98*, 11597−11609.

(19) Van Lent, B.; Scheutjens, J. M. H. M. *Macromolecules* **1989**, *22*, 1931−1937.

(20) Timmermans, J. *Physico-Chemical Constants of Pure Organic Compounds*; American Elsevier: New York, 1950 (Vol. I) and 1965 (Vol. II).

(21) Boublink, T., Fried, V.; Hala, E. In *Physical Sciences Data 17*; Elsevier: Amsterdam, 1984.

(22) Lide, D. R. *CRC Handbook of Chemistry and Physics*; CRC Press Inc.: Boca Raton, FL, 1992−1993.

(23) Anselme, M. J., Gude, M.; Teja, A. S. *Fluid Phase Equilib.* **1990**, *57*, 317−326.

(24) Barneveld, P. A., Scheutjens, J. M. H. M.; Lyklema, J. *Langmuir* **1992**, *8*, 3122−3130.

(25) Weber, T. A. *J. Chem. Phys.* **1980**, *72*, 4014−4018.

(26) Jasper, J. J.; Kring, E. V. *J. Phys. Chem* **1955**, *59*, 1019−1021.

(27) Earnshaw, J. C.; Hughes, C. J. *Phys. Rev. A.* **1992**, *46*, R4494-R4496.

(28) Wu, X. Z., Ocko, B. M., Sirota, E. B., Sinha, S. K.; Deutsch, M. *Physica A* **1993**, *200*, 751−758.

(29) Leermakers, F. A. M.; Cohen Stuart, M. A. *Phys. Rev. Lett.* **1996**, *76*, 82−85.

(30) Meijer, L. A., Leermakers, F. A. M.; Nelson, A. *Langmuir* **1994**, *10*, 1199−1206.

(31) Legrand, D. G.; Gaines, G. L. *J. Colloid Interface Sci.* **1969**, *31*, 162−167.

(32) Schlangen, L. J. M. *Adsorption and Wetting, experiments, thermodynamics and molecular aspects*, Ph.D Thesis, Wageningen Agricultural University, Wageningen, The Netherlands, 1995.

(33) Schlangen, L. J. M., Leermakers, F. A. M.; Koopal, L. K. *Faraday Trans.*, Modern Techniques for the Study of Wet Interfaces (special issue), in press.

(34) Schlangen, L. J. M.; Koopal, L. K. *Langmuir*, in press.

JP9504635